Coherent control of negative refraction based on local-field enhancement and dynamically induced chirality*

Ba Nuo(巴 诺), Gao Jin-Wei(高金伟), Tian Xing-Xia(田杏霞), Wu Xi(吴 熙), and Wu Jin-Hui(吴金辉)†

College of Physics, Jilin University, Changchun 130023, *China*

(Received 18 August 2009; revised manuscript received 14 December 2009)

This paper studies the electromagnetic response of a coherently driven dense atomic ensemble to a weak probe. It finds that negative refraction with little absorption may be achieved in the presence of local-field enhanced interaction and dynamically induced chirality. The complex refractive index governing the probe refraction and absorption depends critically on the atomic density, the steady population distribution, the coherence dephasings, and the frequency detunings, and is also sensitive to the phase of the driving field because the photonic transition paths form a close loop. Thus, it can periodically tune the refractive index at a fixed frequency from negative to positive values and vice versa just by modulating the driving phase. Moreover, the optimal negative refraction is found to be near the probe magnetic resonance, which then requires the electric fields of the probe and the drive being on two-photon resonance due to the dipole synchronisation.

Keywords: negative refraction, dynamically induced chirality, local field enhancement, electromagnetically induced transparency

PACC: 4250, 3280

1. Introduction

Inspired by the pioneering work of Pendry *et al.* 10 years ago,[1] materials of negative refraction have become an active area of research due to their counterintuitive electromagnetic properties and their potential applications.[2]. In such peculiar materials, for example, the phase velocity of an electromagnetic wave and its energy flow are in the opposite directions, and a perfect lens could be developed with its imaging resolution not restricted by the wavelength.[3] Negative refraction materials, first introduced as left-handed media by Veselago in the 1960s,[4] usually possess both negative electric permittivity $\varepsilon_{\rm r}$ and negative magnetic permeability $\mu_{\rm r}$ in a certain frequency band. Recently it was shown that, however, negative refraction of electromagnetic waves could be achieved in the so-called chiral materials without requiring both negative $\varepsilon_{\rm r}$ and negative $\mu_{\rm r}$.[5] In a chiral medium, the refractive index n also depends on two chirality coefficients ξ_{EH} and ξ_{HE} because the polarisation P is coupled with the magnetic field H of an electromagnetic wave and the magnetisation M is coupled with its electric field E.

So far, several interesting approaches have been proposed to realise negative refraction, among which the method using artificial composite metamaterials[6,7] and the method using specific photonic crystals[8,9] are the most popular ones. Negative refraction in the microwave region has been experimentally demonstrated with a periodic structure composed of split-ring resonators and conducting wires,[10] and the refractive index may be tuned between negative and positive values by modulating certain characteristics of the involved metamaterials.[11,12] To realise negative refraction in the optical region, one can resort to another method depending on quantum coherence established in dense atoms with notable local fields by applying laser fields on appropriate energy levels.[13−19] In particular, Kastel *et al.* show that the chirality based on dynamically induced coherence may result in negative refraction with very low absorption in the optical region.[20,21] This method may be regarded as a modified version of the well-known electromagnetically induced transparency (EIT) technique,[22−25] where the dilute atoms are made highly transparent and dispersive to a weak probe in a narrow frequency window by a moderate

*Project supported by the National Natural Science Foundation of China (Grant No. 10874057).

†Corresponding author. E-mail: jhwu@jlu.edu.cn

© 2010 Chinese Physical Society and IOP Publishing Ltd

driving field.

In this paper, we investigate how to achieve and control the negative refraction in a dense atomic ensemble with local-field effects by providing detailed treatments on the complex refractive index. It is shown that the negative refraction accompanied by a transparency window can be attained as the probe and driving fields induce notable chirality in the dense atoms with a close-loop transition path. The spectral curves describing the probe refraction and absorption change dramatically as one varies the steady population at the two lowest levels, which tells us that the two chirality coefficients are critical for the negative refraction, the electric susceptibility answers for the transparency window, while the magnetic susceptibility is negligibly small. This could be better understood if we decompose the close-loop atomic system into two coupled three-level EIT systems sharing the same driving electric field but utilising the probe electric and magnetic transitions, respectively. In addition, the magnetic dephasing rate on the two-photon transition in one EIT system should be kept very small to have notable transparency and negative refraction. If this dephasing rate is not small enough, one can increase the driving Rabi frequency to suppress the absorption and use a denser atomic ensemble to enhance the negative refraction. The probe response is also found to be sensitive to the driving phase in a periodic mode, which is one important characteristic of any close-loop atomic systems. The phase control technique has been explored to manipulate single-atom spontaneous emission, light amplification without inversion, collective quantum dynamics, etc.[26−30] Finally we note that the requirement of dipole synchronisation can be fulfilled even if the probe electric and magnetic transitions are different in frequency, and the negative refraction with little absorption is near the probe magnetic transition when the electric fields of the probe and driving are on two-photon resonance.

2. Model and method

We show the close-loop atomic system interacting with a strong driving field $\omega_{\rm c}$ and a weak probe field $\omega_{\rm p}$ in Fig. 1, where levels $|1\rangle$, $|2\rangle$, and $|3\rangle$ are opposite to level $|4\rangle$ in parity and the frequency difference between levels $|4\rangle$ and $|3\rangle$ is approximately equal to that between levels $|2\rangle$ and $|1\rangle$. Then the electric and magnetic components of the weak probe, $E_{\rm p}$ and $B_{\rm p}$,

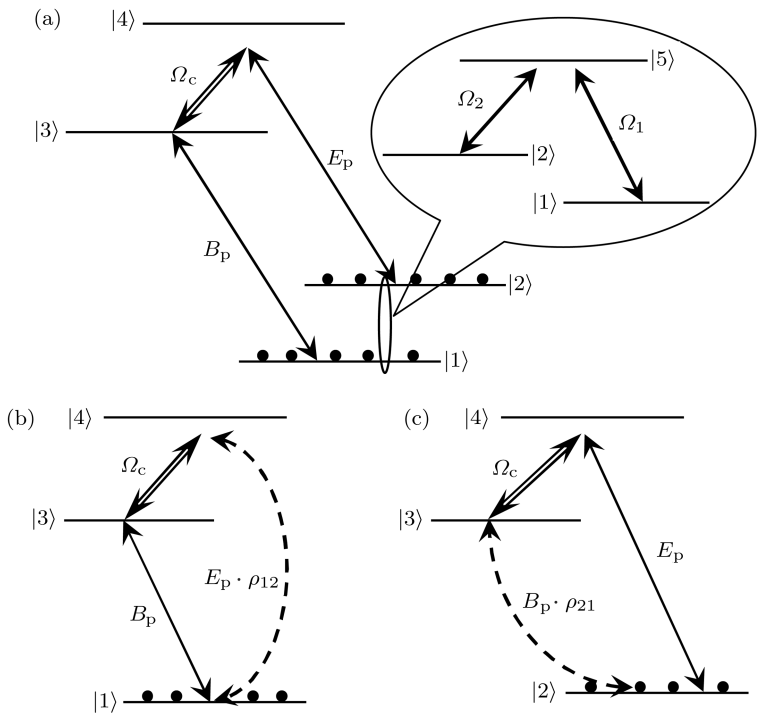


Fig. 1. (a) Schematic diagram of a five-level atomic system with a close-loop transition path. In the weak probe limit, one can reasonably eliminate level $|5\rangle$ together with the two assistant fields by assuming a dark state composed of levels $|1\rangle$ and $|2\rangle$. (b) and (c) Two three-level atomic systems decomposed from the five-level close-loop one and coupled through the common coherence term ρ_{12}.

will drive transitions $|4\rangle \leftrightarrow |2\rangle$ and $|3\rangle \leftrightarrow |1\rangle$ through the electric- and magnetic-dipole interactions, respectively. In the limit of a weak probe, almost all population will be distributed at the two lowest levels $|1\rangle$ and $|2\rangle$ (i.e. $\rho_{11} + \rho_{22} = 1$) as a result of the severe unbalance between atomic decay and pumping. In the following, we assume that this two levels be in a dark state $|\Psi_{\rm d}\rangle = [\Omega_2 |1\rangle - \Omega_1 |2\rangle]/\sqrt{\Omega_1^2 + \Omega_2^2}$,[31,32] where $\Omega_1 = E_1 d_{51}/2\hbar$ and $\Omega_2 = E_2 d_{52}/2\hbar$ are Rabi frequencies of the two laser fields acting on the assistant transitions $|5\rangle \leftrightarrow |1\rangle$ and $|5\rangle \leftrightarrow |2\rangle$. This assumption allows us to pursue optimal results by modulating contributions of the electric and magnetic transitions $|4\rangle \leftrightarrow |2\rangle$ and $|3\rangle \leftrightarrow |1\rangle$ to the probe response.

With the rotating-wave approximation, under the assumption of $\hbar = 1$, the interaction Hamiltonian can be expressed as

$$H_I = \begin{pmatrix} 0 & 0 & \Omega_B & 0 \\ 0 & \Delta_B + \Delta_{\rm c} - \Delta_E & 0 & \Omega_E \\ \Omega_B & 0 & \Delta_B & \Omega_{\rm c}\,{\rm e}^{-{\rm i}\Phi} \\ 0 & \Omega_E & \Omega_{\rm c}\,{\rm e}^{{\rm i}\Phi} & \Delta_B + \Delta_{\rm c} \end{pmatrix}, \tag{1}$$

where $\Delta_{\rm c} = \omega_{\rm c} - \omega_{43}$, $\Delta_E = \omega_{\rm p} - \omega_{42}$, and $\Delta_B = \omega_{\rm p} - \omega_{31}$ are detunings of the driving and the probe from relevant transitions, while $\Omega_{\rm c} = E_{\rm c} d_{43}/2\hbar$, $\Omega_E = E_{\rm p} d_{42}/2\hbar$, and $\Omega_B = B_{\rm p}\mu_{31}/2\hbar$ are real-valued Rabi frequencies of the corresponding fields. Moreover, Φ denotes the time-independent phase of the driving field, which only makes sense in a close-loop atomic system.

Expanding the well-known Liouville equation in this atomic system, we derive the following equations for nonzero density matrix elements

$$\begin{aligned}
\frac{\partial \rho_{13}}{\partial t} &= -[\gamma_{13} + {\rm i}\Delta_B]\rho_{13} - {\rm i}\Omega_{\rm c}\,{\rm e}^{{\rm i}\Phi}\rho_{14} - {\rm i}\Omega_B\rho_{11}, \\
\frac{\partial \rho_{14}}{\partial t} &= -\left[\gamma_{14} + {\rm i}(\Delta_B + \Delta_{\rm c})\right]\rho_{14} - {\rm i}\Omega_{\rm c}\,{\rm e}^{-{\rm i}\Phi}\rho_{13} \\
&\quad - {\rm i}\Omega_E\rho_{12}, \\
\frac{\partial \rho_{23}}{\partial t} &= -[\gamma_{23} + {\rm i}(\Delta_E - \Delta_{\rm c})]\rho_{23} - {\rm i}\Omega_B\rho_{21} \\
&\quad - {\rm i}\Omega_{\rm c}\,{\rm e}^{{\rm i}\Phi}\rho_{24}, \\
\frac{\partial \rho_{24}}{\partial t} &= -\left[\gamma_{24} + {\rm i}\Delta_E\right]\rho_{24} - {\rm i}\Omega_{\rm c}\,{\rm e}^{-{\rm i}\Phi}\rho_{23} \\
&\quad - {\rm i}\Omega_E\rho_{22},
\end{aligned} \tag{2}$$

with the assumption of $\rho_{33} = \rho_{44} = \rho_{34} = 0$ in the weak probe limit. Here $\gamma_{ij} = \left[\sum_k (\Gamma_{ik} + \Gamma_{jk})\right]/2$ denotes the dephasing rate of atomic coherence ρ_{ij} with Γ_{ij} being the population decay rate from level $|i\rangle$ to level $|j\rangle$. We note that the dipole synchronisation requires the frequency degeneracy condition of $\omega_{\rm p} + \omega_{\rm c} - \omega_{\rm p} = \omega_{31} + \omega_{43} - \omega_{42} = \omega_{21}$, i.e. $\Delta_B + \Delta_{\rm c} - \Delta_E = 0$, which implies that the probe is not necessary to be simultaneously resonant with transitions $|3\rangle \leftrightarrow |1\rangle$ and $|4\rangle \leftrightarrow |2\rangle$.

Equation (2) characterises in fact two coupled EIT systems mediated by the coherence term ρ_{12}: one is in the Ladder configuration [see Fig. 1(b)] described by the first two equations, while the other is in the Lambda configuration [see Fig. 1(c)] described by the last two equations. In the Ladder system, the probe magnetic transition $|1\rangle \leftrightarrow |3\rangle$ can be finished through either the direct coupling of $B_{\rm p}$ or the cross coupling of $\rho_{12} \cdot E_{\rm p} \cdot \Omega_{\rm c}$. Similarly, the probe electric transition $|2\rangle \leftrightarrow |4\rangle$ in the Lambda system also have two paths: the direct coupling one bridged by $E_{\rm p}$ and the cross coupling one bridged by $\rho_{21} \cdot B_{\rm p} \cdot \Omega_{\rm c}$. These four transition paths are expected to interact and interfere to give surprising and interesting results on the probe response in some situations.

The steady-state solutions of Eq. (2) can be easily attained by the perturbation method if ρ_{11}, ρ_{22}, and ρ_{12} are fully determined by Rabi frequencies Ω_1 and Ω_2 of the two assistant fields. To the first order of Ω_E and Ω_B, the two coherence terms ρ_{31} and ρ_{42} governing the probe response are derived as

$$\begin{aligned}
\rho_{42}^{(1)} &= \alpha_{EE} E_{\rm p} + \alpha_{EH} B_{\rm p}, \\
\rho_{31}^{(1)} &= \alpha_{HE} E_{\rm p} + \alpha_{HH} B_{\rm p},
\end{aligned} \tag{3}$$

where

$$\begin{aligned}
\alpha_{EE} &= \frac{{\rm i} d_{42}\rho_{22}\left[\gamma_{23} - {\rm i}\left(\Delta_E - \Delta_{\rm c}\right)\right]}{2\hbar\{\left[\gamma_{23} - {\rm i}\left(\Delta_E - \Delta_{\rm c}\right)\right]\left(\gamma_{24} - {\rm i}\Delta_E\right) + \Omega_{\rm c}^2\}}, \\
\alpha_{EH} &= \frac{-\mu_{31}\rho_{12}\Omega_{\rm c}\,{\rm e}^{+{\rm i}\Phi}}{2\hbar\{\left[\gamma_{23} - {\rm i}\left(\Delta_E - \Delta_{\rm c}\right)\right]\left(\gamma_{24} - {\rm i}\Delta_E\right) + \Omega_{\rm c}^2\}}, \\
\alpha_{HH} &= \frac{{\rm i}\mu_{31}\rho_{11}\left[\gamma_{14} - {\rm i}\left(\Delta_B + \Delta_{\rm c}\right)\right]}{2\hbar\{\left[\gamma_{14} - {\rm i}\left(\Delta_B + \Delta_{\rm c}\right)\right]\left(\gamma_{13} - {\rm i}\Delta_B\right) + \Omega_{\rm c}^2\}}, \\
\alpha_{HE} &= \frac{-d_{42}\rho_{21}\Omega_{\rm c}\,{\rm e}^{-{\rm i}\Phi}}{2\hbar\{\left[\gamma_{14} - {\rm i}\left(\Delta_B + \Delta_{\rm c}\right)\right]\left(\gamma_{13} - {\rm i}\Delta_B\right) + \Omega_{\rm c}^2\}},
\end{aligned}$$

with the α_{EE} and α_{HH} being the polarizability parameters resulted from the direct couplings while α_{EH} and α_{HE} are the chirality parameters due to the cross couplings. From Eq. (3), we can further determine the polarisation $P = N d_{24}\rho_{42}$ and the magnetisation $M = N\mu_{13}\rho_{31}$ for the whole atomic ensemble with N being its density. For chiral materials we also have

$$P = \varepsilon_0\chi_e E_{\rm p} + \frac{\xi_{EH} H_{\rm p}}{c},$$

$$M = \frac{\xi_{HE} E_{\rm p}}{c\mu_0} + \chi_m H_{\rm p}, \tag{4}$$

with χ_e, χ_m, ξ_{EH}, and ξ_{HE} being the electric susceptibility, the magnetic susceptibility, and the two chirality coefficients, respectively. Thus χ_e, χ_m, ξ_{EH}, and ξ_{HE} may be obtained with Eqs. (3) and (4) as

$$\begin{aligned}
\chi_e &= \frac{{\rm i}N\left|d_{24}\right|^2 \rho_{22}\left[\gamma_{23} - {\rm i}\left(\Delta_E - \Delta_{\rm c}\right)\right]}{2\hbar\varepsilon_0\{\left[\gamma_{23} - {\rm i}\left(\Delta_E - \Delta_{\rm c}\right)\right]\left(\gamma_{24} - {\rm i}\Delta_E\right) + \Omega_{\rm c}^2\}},\\
\xi_{EH} &= \frac{-Nd_{24}(\mu_{31}/c)\rho_{12}\Omega_{\rm c}\,{\rm e}^{+{\rm i}\Phi}}{2\hbar\varepsilon_0\{\left[\gamma_{23} - {\rm i}\left(\Delta_E - \Delta_{\rm c}\right)\right]\left(\gamma_{24} - {\rm i}\Delta_E\right) + \Omega_{\rm c}^2\}},\\
\chi_m &= \frac{{\rm i}N\left|\mu_{13}/c\right|^2 \rho_{11}\left[\gamma_{14} - {\rm i}\left(\Delta_B + \Delta_{\rm c}\right)\right]}{2\hbar\varepsilon_0\{\left[\gamma_{14} - {\rm i}\left(\Delta_B + \Delta_{\rm c}\right)\right]\left(\gamma_{13} - {\rm i}\Delta_B\right) + \Omega_{\rm c}^2\}},\\
\xi_{HE} &= \frac{-N(\mu_{13}/c)d_{42}\rho_{21}\Omega_{\rm c}\,{\rm e}^{-{\rm i}\Phi}}{2\hbar\varepsilon_0\{\left[\gamma_{14} - {\rm i}\left(\Delta_B + \Delta_{\rm c}\right)\right]\left(\gamma_{13} - {\rm i}\Delta_B\right) + \Omega_{\rm c}^2\}}.
\end{aligned} \tag{5}$$

If the atomic ensemble is very dense, however, we have to take into account both electric and magnetic local-field effects, i.e. to replace the macroscopic $E_{\rm p}$ and $B_{\rm p}$ in Eq. (3) with the microscopic $E_m = E_{\rm p} + P/3\varepsilon_0$ and $B_m = B_{\rm p} + \mu_0 M/3$. In this case, the four direct and cross coupling coefficients are instead given by

$$\begin{aligned}
\chi_e' &= \frac{9\chi_e - 3(\chi_e\chi_m - \xi_{EH}\xi_{HE})}{9 - 3\chi_m - 3\chi_e + \chi_e\chi_m - \xi_{EH}\xi_{HE}},\\
\xi_{EH}' &= \frac{9\xi_{EH}}{9 - 3\chi_m - 3\chi_e + \chi_e\chi_m - \xi_{EH}\xi_{HE}},\\
\chi_m' &= \frac{9\chi_m - 3(\chi_e\chi_m - \xi_{EH}\xi_{HE})}{9 - 3\chi_m - 3\chi_e + \chi_e\chi_m - \xi_{EH}\xi_{HE}},\\
\xi_{HE}' &= \frac{9\xi_{HE}}{9 - 3\chi_m - 3\chi_e + \chi_e\chi_m - \xi_{EH}\xi_{HE}}.
\end{aligned} \tag{6}$$

Using these modified coefficients, we can finally determine the complex refractive index through

$$n = \sqrt{\varepsilon_{\rm r}\mu_{\rm r} - \frac{\left(\xi_{EH}' + \xi_{HE}'\right)^2}{4}} + \frac{{\rm i}\left(\xi_{EH}' - \xi_{HE}'\right)}{2}, \tag{7}$$

with $\varepsilon_{\rm r} = 1+\chi_e'$ and $\mu_{\rm r} = 1+\chi_m'$ being the electric permittivity and the magnetic permeability respectively. Note that the complex square root in Eq. (7) has two solutions with a phase difference of π, but we just need to use the one guaranteeing a positive Im(n) in calculation. This is because the probe should not be amplified when all atoms are populated into the lowest levels $|1\rangle$ and $|2\rangle$. Then we can examine how to achieve and control the negative refraction by modulating the relevant atomic and electromagnetic parameters.

3. Results and discussions

We first discuss the importance of dynamically induced chirality for achieving negative refraction by changing the steady population at levels $|1\rangle$ and $|2\rangle$. From Fig. 2 we can see that the negative refraction are obtained around a transparency window with appropriately chosen parameters. In particular, the maximal magnitude of negative refraction corresponds to the case of $\rho_{11} = \rho_{22} = -\rho_{12} = 0.5$ where the chirality coefficients ξ_{EH} and ξ_{HE} have the largest absolute values. As we gradually decrease ρ_{11}, the transparency window in the Im(n) curve becomes narrower and the negative-valued part of the Re(n) curve tends to the zero line. In this case, the electric susceptibility χ_e is enhanced while the magnetic susceptibility χ_m and the two chirality coefficients ξ_{EH} and ξ_{HE} are weakened. In the ultimate situation of $\rho_{11} = 0$, the transparency window is narrowest and no negative refraction exists around it as a result of $\chi_m = \xi_{EH} = \xi_{HE} = 0$. Conversely, if we increase ρ_{11} starting from the balanced case of $\rho_{11} = 0.5$, the negative-valued part of the Re(n) curve once again tends to the zero line, but the transparency window becomes wider instead of narrower. In this case, the enhanced susceptibility is the magnetic one χ_m but not the electric one χ_e. Finally, we find that Im(n)$\equiv 0$ and Re(n)$\equiv 1$ when χ_m gets the largest absolute value and $\chi_e = \xi_{EH} = \xi_{HE} = 0$ in the ultimate situation of $\rho_{11} = 1$. Thus we may conclude that: (a) the direct coupling coefficient χ_m in the Ladder EIT system is always negligible for the probe response; (b) the direct coupling coefficient χ_e in the Lambda EIT system answers for the probe transparency; (c) the cross coupling coefficients ξ_{EH} and ξ_{HE} are critical for achieving the negative refraction around a transparency window.

In the above, we have chosen identical dephasings for the two electric transitions ($\gamma_{14} = \gamma_{24}$) but different dephasings for the two magnetic transitions ($\gamma_{13} \gg \gamma_{23}$). The larger γ_{13} in the Ladder EIT system may also be contributed by, e.g. the laser linewidth, except the population decay. The smaller γ_{23} in the Lambda EIT system is assumed to only originate from the population decay because it corresponds to a two-photon transition where the laser linewidth can be well eliminated via phase locking. Moreover, we have set $\gamma_{14} = \gamma_{24} = (137)^2\gamma_{23}$ because the electric- and magnetic-dipole elements are related to the decay rates through $d_{24} = \sqrt{3\pi\varepsilon_0\gamma_{24}\hbar c^3/\omega_{24}^3}$ and $\mu_{13}/c = \sqrt{3\pi\varepsilon_0\gamma_{13}\hbar c^3/\omega_{13}^3}$, respectively.[20]

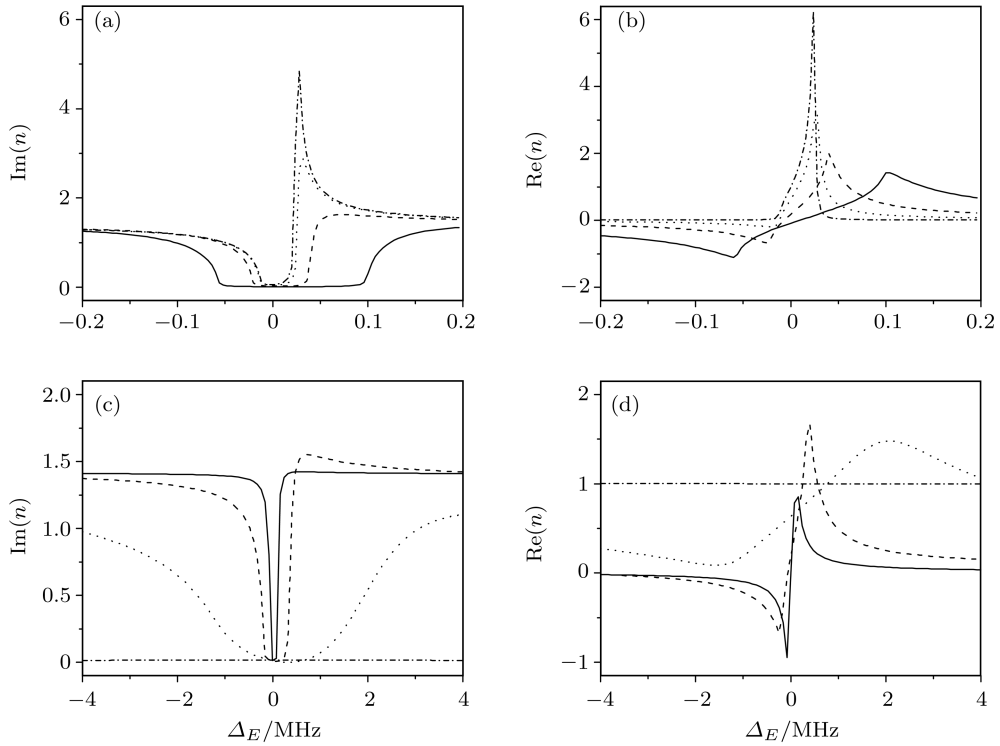


Fig. 2. Imaginary (a, c) and real (b, d) parts of the refractive index as a function of the probe detuning. In figures (a) and (b), the solid, dashed, dotted, dash-dotted curves respectively correspond to $\rho_{11} = 0.5$, 0.1, 0.01, and 0. In figures (c) and (d), the solid, dashed, dotted, dash-dotted curves respectively correspond to $\rho_{11} = 0.5$, 0.9, 0.99, and 1.0. Other parameters are $\gamma_{23} = 1.0$ kHz, $\gamma_{13} = 10.0$ MHz, $\gamma_{24} = \gamma_{14} = 137^2\gamma_{23}$, $\Omega_c = 8.0$ MHz, $\Delta_0 = 0$, $\Phi = \pi/2$, and $N = 1.0 \times 10^{23}$ m^{-3}.

Considering that γ_{23} may have a larger value, we examine in Fig. 3 the real and imaginary parts of the complex refractive index with different values of γ_{23}. Clearly the probe absorption becomes more and more severe and the maximal magnitude of negative refraction becomes smaller and smaller as one gradually increases γ_{23}. In particular, no negative refraction and transparency window can be found when $\gamma_{23} \geq 1.0$ MHz. This once again verifies that the electric susceptibility χ_e in the Lambda EIT system, which is very sensitive to γ_{23}, mainly contributes to the transparency window. Thus one can suppress the residual absorption in the transparency window by increasing the driving Rabi frequency Ω_c (compare the solid and dashed curves in Fig. 4). To simultaneously enhance the negative refraction, we also need to increase the atomic density N, which then induces a little more absorption (compare the dashed and dotted curves in Fig. 4). Anyway, we can achieve notable negative refraction accompanied with little absorption by increasing both Ω_c and N in the case of a larger γ_{23}.

Then what about the other magnetic dephasing γ_{13}? Figure 5 shows that, when $\gamma_{13} \geq 0.1$ MHz, a smaller γ_{13} corresponds to a larger magnitude of negative refraction and a wider and deeper transparency window. If $\gamma_{13} \leq 0.1$ MHz, however, the Im(n) and Re(n) curves seem that there is no change as one gradually vary γ_{13}. Comparing Fig. 3 with Fig. 5, we can see that γ_{13} is not as important as γ_{23} because γ_{13} affects n only through ξ_{HE} (χ_m is always neglectable) while γ_{23} affects n through both χ_e and ξ_{EH}. In other words, the Lambda EIT system dealing with the probe electric transition plays a more important role than the Ladder EIT system dealing with the probe magnetic transition. Moreover, we have chosen $\Delta_B - \Delta_E = \Delta_0 = 5.0$ MHz in Fig. 5, which then requires $\Delta_c = -\Delta_0 = -5.0$ MHz due to the dipole synchronisation. In this case, the negative refraction and the transparency window are observed near $\Delta_E = -5.0$ MHz, i.e. near $\Delta_B = 0$. Thus, the basic requirement for achieving negative refraction with little absorption is: (a) the probe is approximately resonant with its magnetic transition; (b) the coupling and the probe are approximately on two-photon resonance through electric transitions.

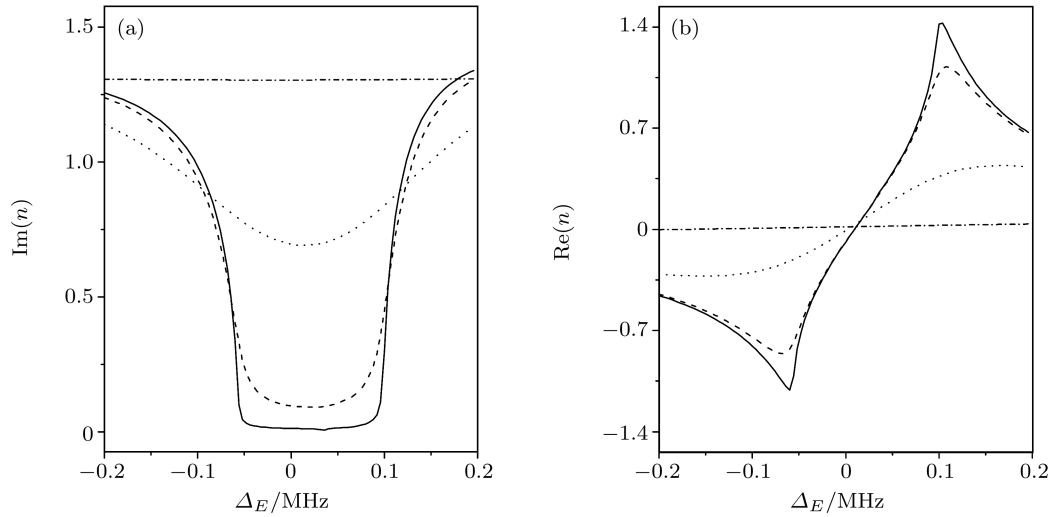


Fig. 3. Imaginary (a) and real (b) parts of the refractive index as a function of the probe detuning for $\gamma_{23} = 1.0$ kHz (solid), $\gamma_{23} = 10.0$ kHz (dashed), $\gamma_{23} = 0.1$ MHz (dotted), and $\gamma_{23} = 1.0$ MHz (dash-dotted), respectively. Other parameters are the same as those in Fig. 2 except $\rho_{11} = 0.5$.

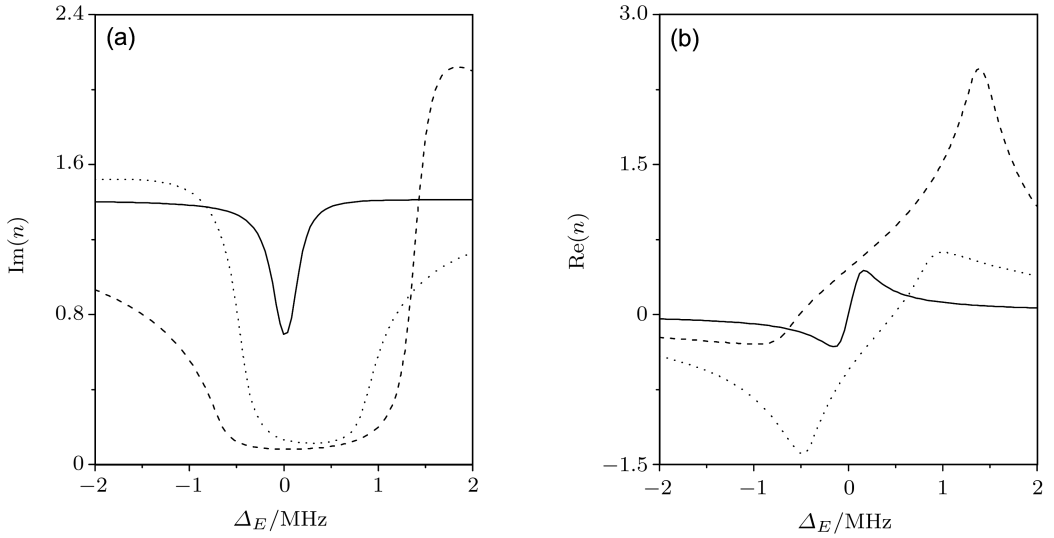


Fig. 4. Imaginary (a) and real (b) parts of the refractive index as a function of the probe detuning for $\Omega_c = 8.0$ MHz and $N = 1.0 \times 10^{23}$ m^{-3} (solid), $\Omega_c = 40.0$ MHz and $N = 1.0 \times 10^{23}$ m^{-3} (dashed), and $\Omega_c = 40.0$ MHz and $N = 5.0 \times 10^{23}$ m^{-3} (dotted), respectively. Other parameters are the same as those in Fig. 2 except $\rho_{11} = 0.5$ and $\gamma_{23} = 0.1$ MHz.

Finally we discuss the dependence of the complex refractive index n on the driving phase Φ, one most important characteristic of the close-loop atomic system. From Eqs. (5)–(7) we can see that ξ_{EH} and ξ_{HE}, and therefore Im(n) and Re(n), are sensitive to the driving phase Φ in a periodic mode, which is just shown in Fig. 6. In particular, we note from Fig. 6 that there exist a series of modes hopping at $\Phi \cong 2k\pi + 0.5\pi$ and $\Phi \cong 2k\pi + 1.5\pi$. If the driving phase is increased from $\Phi \cong 2k\pi + 0.5\pi$ to $\Phi \cong 2k\pi + 1.5\pi$ (from $\Phi \cong 2k\pi + 1.5\pi$ to $\Phi \cong 2k\pi + 2.5\pi$), the refractive index Re(n) at $\Delta_E = -0.4$ MHz will change from negative to positive values (from positive to negative values). The refractive index Re(n) at $\Delta_E = 0.8$ MHz, however, varies in the reverse direction for the same driving phase modulation. That is, we can manipulate the refractive index Re(n) at a fixed frequency via the periodic phase modulation. To well suppress the probe absorption as attaining the negative refraction at $\Delta_E = -0.4$ MHz and $\Delta_E = 0.8$ MHz, however, we should carefully set the driving phase near $\Phi = k\pi + 0.5\pi$.

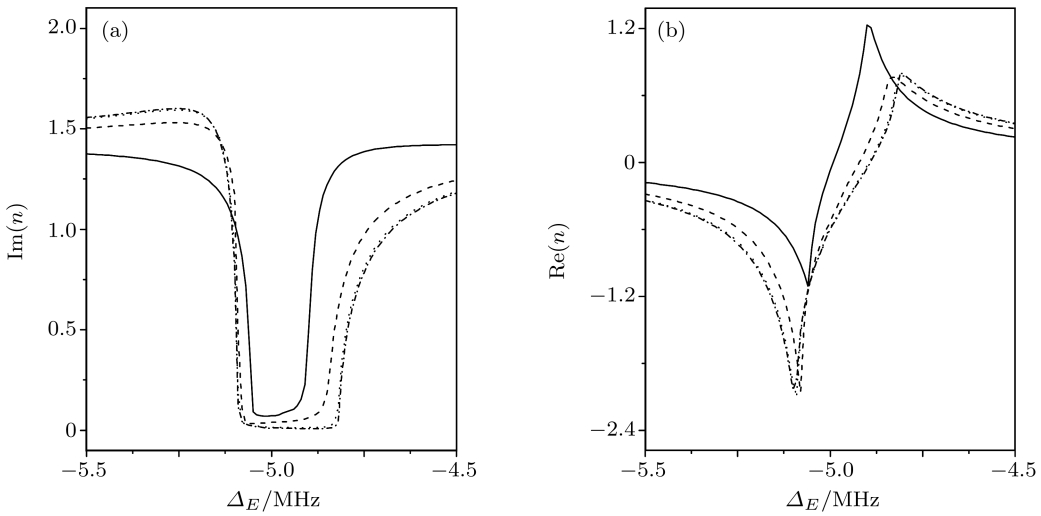


Fig. 5. Imaginary (a) and real (b) parts of the refractive index as a function of the probe detuning for $\gamma_{13} = 10.0$ MHz (solid), $\gamma_{13} = 1.0$ MHz (dashed), $\gamma_{13} = 0.1$ MHz (dotted), and $\gamma_{13} = 0.01$ MHz (dash-dotted), respectively. Other parameters are the same as those in Fig. 2 except $\rho_{11} = 0.5$ and $\Delta_0 = 5.0$ MHz.

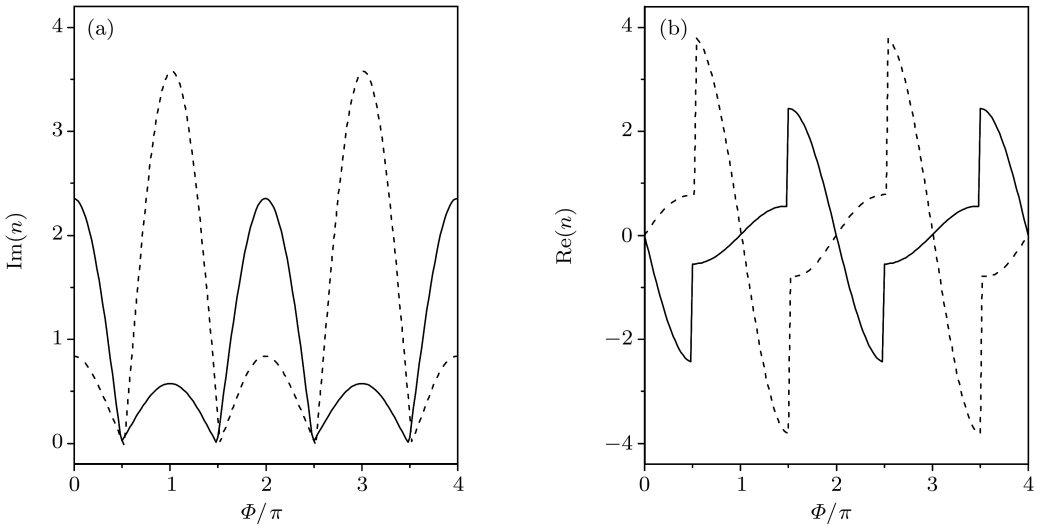


Fig. 6. Imaginary (a) and real (b) parts of the refractive index as a function of the driving phase for $\Delta_E = -0.4$ MHz (solid) and $\Delta_E = 0.8$ MHz (dashed), respectively. Other parameters are the same as those in Fig. 2 except $\rho_{11} = 0.5$.

4. Conclusion

In summary, we have studied a close-loop atomic system for achieving negative refraction in the optical region by considering the specific situation where the probe is simultaneously near resonant with an electric transition and a magnetic transition. In case the atomic ensemble is dense enough to bear notable local-field effects, the negative refraction accompanied with a transparency window is viable to be attained with the dynamically induced chirality. The close-loop atomic system may be decomposed into two correlated three-level EIT systems respectively regarding the probe electric and magnetic transitions. In each EIT system, there exist a direct coupling term (the electric susceptibility χ_e or the magnetic susceptibility χ_m) and a cross coupling term (the chirality coefficient ξ_{EH} or ξ_{HE}) relevant to the probe response, which may be controlled by varying the steady population at the two lowest levels. We find that the transparency window is mainly contributed by the electric susceptibility, while keys for achieving negative refraction are the two chirality coefficients. Moreover, the magnetic dephasing rate γ_{23} in one EIT system should

be very small, otherwise the transparency window and the negative refraction may not be observed. But we can reduce the absorption and enhance the negative refraction by increasing the driving Rabi frequency Ω_c and the atomic density N at the same time. It is worth noting that we also can periodically tune the refractive index between positive and negative values by modulating the driving phase Φ, while the negligible absorption can only be obtained with $\Phi \cong k\pi + 0.5\pi$. Last but not least, the negative refraction and the transparency window are always near the probe magnetic resonance when the probe and driving electric fields are on two-photon resonance as required by the dipole synchronisation.

Our work should be instructive for choosing appropriate atoms or molecules with excellent optical parameters to achieve negative refraction with little absorption in the optical region.

References

[1] Pendry J B, Holden A J, Robbins D J and Stewart W J 1999 *IEEE Trans. Microwave Theory Tech.* **47** 2075
[2] Ramakrishna S A 2005 *Rep. Prog. Phys.* **68** 449
[3] Pendry J B 2000 *Phys. Rev. Lett.* **85** 3966
[4] Veselago V G 1968 *Sov. Phys. Usp.* **10** 509
[5] Pendry J B 2004 *Science* **306** 1353
[6] Yannopapas V and Moroz A 2005 *J. Phys.*: *Condens. Matter* **17** 3717
[7] Wheeler M S, Aitchison J S and Mojahedi M 2005 *Phys. Rev.* B **72** 193103
[8] He S L, Ruan Z C, Chen L and Shen J Q 2004 *Phys. Rev.* B **70** 115113
[9] Thommen Q and Mandel P 2006 *Opt. Lett.* **31** 1803
[10] Shelby R A, Smith D R and Schultz S 2001 *Science* **297** 77
[11] Werner D H, Kwon D and Khoo I 2007 *Opt. Express* **15** 3342
[12] Wang X D, Kwon D H, Werner D H, Khoo L C, Kildisher A V and Shalaev V M 2007 *Appl. Phys. Lett.* **91** 143122
[13] Shen J Q, Ruan Z C and He S L 2004 *J. Zhejiang Univ. Sci.* **5** 1322
[14] Oktel M Ö and Müstecaplioğlu Ö E 2004 *Phys. Rev.* A **70** 053806
[15] Thommen Q and Mandel P 2006 *Phys. Rev. Lett.* **96** 053601
[16] Zhang H J, Niu Y P and Gong S Q 2006 *Phys. Lett.* A **363** 497
[17] Shen J Q 2007 *Chin. Phys.* **16** 1976
[18] Zheng J, Liu Z D, Zeng F H and Fang H J 2008 *Acta Phys. Sin.* **57** 4219 (in Chinese)
[19] Ba N, Gao J W, Fan W, Wang D W, Ma Q R, Wang R and Wu J H 2008 *Opt. Commun.* **281** 5566
[20] Kastel J, Fleischhauer M, Yelin S F and Walsworth R L 2007 *Phys. Rev. Lett.* **99** 073602
[21] Zhang H J, Niu Y P, Sun H, Luo J and Gong S Q 2008 *J. Phys.* B **41** 125503
[22] Harris S E 1997 *Phys. Today* **50** 36
[23] Fleischhauer M, Imamoglu A and Marangos J P 2005 *Rev. Mod. Phys.* **77** 633
[24] Yang L J, Zhang L S, Li X L, Li X W, Guo Q L, Han L and Fu G S 2006 *Acta Phys. Sin.* **55** 5206 (in Chinese)
[25] Jia W Z and Wang S J 2009 *Chin. Phys.* B **18** 2282
[26] Quang T, Woldeyohannes M, Sajeev J and Agarwal G S 1997 *Phys. Rev. Lett.* **79** 5238
[27] Wu J H and Gao J Y 2002 *Phys. Rev.* A **65** 063807
[28] Macovei M, Evers J and Keitel C H 2003 *Phys. Rev. Lett.* **91** 233601
[29] Cui N, Fan X J, Li A Y, Liu C P, Gong S Q and Xu Z Z 2007 *Chin. Phys.* **16** 718
[30] Yang Y L, Liu Z B, Wang L, Tong D M and Fan X J 2009 *Chin. Phys.* B **18** 1054
[31] Gray H R, Whitley R M and Stroud Jr C R 1978 *Opt. Lett.* **3** 218
[32] Arimondo E 1996 *Coherent Population Trapping in Laser Spectroscopy* In: Wolf E (editor) *Progress in Optics* XXXV (Amsterdam: Elsevier Science) p257